Composite Structures 351 (2025) 118589

Contents lists available at ScienceDirect

Composite Structures

journal homepage: www.elsevier.com/locate/compstruct

Effect of ply misalignment on the notched strength of composite laminates

O. Vallmajó [a,*], M. Descamps [a], A. Arteiro [b,c], A. Turon [a]

[a] AMADE, Polytechnic School, University of Girona, C/Universitat de Girona 4, 17003 Girona, Spain
[b] DEMec, Faculdade de Engenharia, Universidade do Porto, Rua Dr. Roberto Frias, 4200-465 Porto, Portugal
[c] INEGI, Rua Dr. Roberto Frias, 400, 4200-465 Porto, Portugal

ARTICLE INFO

Keywords:
Composites
Ply deviation
Open hole strength
Multi-fidelity
Finite fracture mechanics
Finite element model

ABSTRACT

Predicting the notched strength of carbon fiber-reinforced polymers is a crucial aspect of composite structure design, particularly when considering the uncertainties stemming from geometric features, material variability and defects. This study focuses on the influence of ply misalignment at the meso-scale level. The research employs a comprehensive methodology to establish notched strength allowables, integrating analytical (low fidelity), which have limitations in the representation of stacking sequence effects and in the generation of ply misalignments, and computational tools (high fidelity), employing a finite element model (FEM). The investigation emphasizes the need for a holistic understanding of these factors to enhance the accuracy of predictions. The results predicted by the analytical and, specially, the numerical models are in good agreement with experimental results. Both models underscore the decrease of the notched strength due to ply misalignment. Finally, a hybrid approach is proposed given that FEM predictions offer more accuracy and a detailed comprehension of the failure mechanisms, while fast analytical models can be used to propagate the uncertainties and to determine the allowables.

1. Introduction

Numerous factors can influence the mechanical performance of composite materials. These include the presence of geometric features, e.g., a hole, the presence of defects, and the intrinsic material variability. Therefore, the design process of composite structures requires a profound understanding of mechanical performance under different loading conditions, while considering the uncertainties arising from the geometrical details, the presence of defects and the material variability. That is why the design process comprises different stages starting from the analysis of the constituents, i.e., micro-scale analysis, progressing to the analysis of small specimens with single or a reduced set of features, i.e., meso-scale analysis, and, finally, culminating with an exhaustive evaluation of more complex designs [1]. In the past, these analyses were primarily conducted through extensive test campaigns. Fortunately, nowadays, there is access to more computational resources and enhanced knowledge for designing composite materials. This includes the use of computational (or high fidelity) models or analytical (or low fidelity) models that account for the correct behavior of these materials.

One of the common design drivers during the qualification of a composite structure is the characterization of the notched strength of fiber-reinforced polymers typically determined from an open-hole (OH) specimen. To mitigate the time and cost constraints associated to extensive testing campaigns, predicting this property can be carried out through analytical or numerical models. Nevertheless, there are many uncertainties that need to be accounted for. Thus, providing a single value is not sufficient to ensure safety. Instead, the generation of design allowables is recommended. Vallmajó et al. [2] introduced a methodology to derive design allowables using a finite fracture mechanics model integrated with Monte Carlo simulations. Following this, Cózar et al. [3] developed an alternative methodology that constructs a response surface to manage situations where obtaining large sample sizes is not reachable. More recently, Catalanotti [4] presented a novel approach for quantifying uncertainty in high-dimensional problems, employing bootstrapping and Bayesian uncertainty quantification techniques. The main sources of variability that have been considered are the intrinsic material uncertainties and the geometric tolerances. However, the presence of manufacturing defects plays a major role on the damage onset and evolution on carbon fiber-reinforced polymers (CFRP), thus on the mechanical performance. One of the most common defects at this scale (meso-scale) is the ply misalignment.

Based on the scale of observation, misalignments can be considered at either ply level or at the individual fiber level, the latter also known as in-plane waviness [5]. This work focuses on defects at the ply level, and consequently, it only considers ply misalignment. It is worth mentioning that, usually, ply misalignment is known as fiber straightness, whose main source of variability is the presence of fiber waviness

* Corresponding author.
E-mail address: oriol.vallmajo@udg.edu (O. Vallmajó).

https://doi.org/10.1016/j.compstruct.2024.118589
Received 18 March 2024; Received in revised form 16 August 2024; Accepted 13 September 2024
Available online 17 September 2024

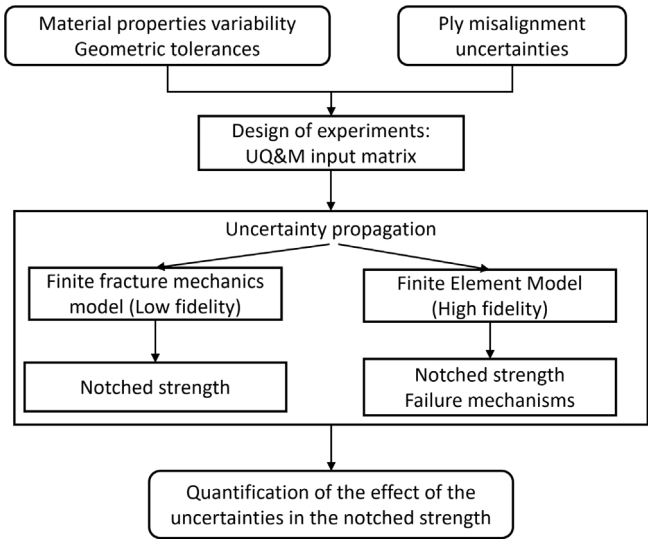

Fig. 1. Flow chart of the propagation of the uncertainties on the notched strength of carbon fiber reinforced polymers.

as reported by Potter et al. [6], or in-plane fiber misalignment [7]. The impact of ply misalignment has been thoroughly investigated in previous research. Hinckley et al. [8] evaluated the effect of ply misalignment using the classical laminated plate theory. Arao et al. [9] assessed the effect of ply misalignment on the out-of-plane deformation of CFRP concluding that ply angle deviation can induce unpredictable out-of-plane deformations. Steeves et al. [10] predicted a similar effect in ultra-thin composite materials. Liu et al. [11] investigated such effect on the out-of-plane deformation of a composite space mirror. Thompson et al. [12] investigated the effect of angular errors during ply placement in uni-directional fiber-polymer composites on the surface deformation peak-to-valley values of circular plates. Cheng et al. [13] examined the effect of ply angle misalignment and thickness deviation on the surface accuracy of CFRP using the classical laminated plate theory and a numerical approach. Tanaka et al. [14] demonstrated that the thermal deformation of CFRP was strongly affected by fiber orientation error. However, to the authors' best knowledge, all the current literature studies have not addressed in detail the effect of uncertainties on ply deviations using approaches with different levels of fidelity.

Therefore, in this work, the effect of ply misalignment and the uncertainties within composite structures are taken into consideration while establishing the notched strength allowable of CFRP using computational and analytical tools.

The paper is organized as follows: Section 2 describes the methodology followed to propagate the uncertainties and determine the notched strength; Section 3 describes the materials considered, the geometry of the specimens as well as the description of the defects; Section 4 presents the results and their discussion; finally, Section 5 summarizes the conclusions of this work.

2. Methodology

The notched strength allowable of a CFRP is calculated using two different approaches: (a) a Finite Fracture Mechanics (FFM) model and (b) a computational model based on the Finite Element Method (FEM). Material variability, the geometric tolerances and the effect of random ply misalignments is considered for both approaches. The flow chart in Fig. 1 shows the strategy followed in this study for the propagation of uncertainties, which is described in the following sections.

2.1. Composite laminate uncertainties

Composite structures have many sources of variability. Due to their inherent orthotropic behavior, the material properties, the geometry and the presence of ply deviations are important factors to consider, as described in the following.

2.1.1. Material properties variability and geometric tolerances

The constituent materials in a composite structure exhibit an intrinsic variability on their properties. Moreover, the processing residual stresses, e.g., due to the chemical shrinkage of the polymer matrix and the mismatch of thermal expansion coefficients between constituents and unidirectional plies of different orientation, and the effect of micro-defects amplify the uncertainties of the meso-scale properties [15]. Therefore, material suppliers and testing labs for material characterization do not provide a single value for the material properties; instead, they provide a mean value and the associated uncertainty, i.e., the statistical distribution or at least the standard deviation (STDV), of the meso-scale properties. This material variability is considered in this study when predicting the notched strength.

Similarly to other homogeneous materials, composite materials are manufactured according to a particular geometry, which, in this study, includes specimens with a hole. However, manufacturing techniques include certain tolerances in the geometry that can potentially influence the material behavior. This study considers the dimensional tolerances of the hole drilled in the specimen and the width of the OH specimen.

2.1.2. Ply misalignment uncertainties

Composite materials exhibit an orthotropic behavior. However, by properly selecting ply angles and stacking sequence, a laminate composed of orthotropic plies can exhibit an isotropic in-plane behavior (quasi-isotropic laminate) or any other tailored (orthotropic or anisotropic) behavior. However, each ply in a laminate may exhibit deviations from the nominal material properties, from the nominal geometry or from the nominal orientation (see Fig. 2) [8]. In particular, the main factors contributing to ply misalignment can be summarized as:

- Imperfections in the alignment of fibers with the edges of the backing material, leading to potential errors in the alignment of templates used for ply cutting.
- Inherent difficulties in aligning and stacking the cut plies during the assembly process, resulting in alignment errors.
- During the curing process, plies may not be fully restrained, allowing for some degree of movement.
- Other defects, such as gaps and overlaps, can also contribute to increased misalignment, as noted by Nguyen et al. [16].

These deviations are likely to be random, normally distributed. However, some deviations, such as errors in the cutting or tape laying machine, would result in a systematic bias in the ply angle deviation [8]. Therefore, this study will take into account both the random deviations in individual plies and the inclusion of a bias factor in the most important load carrying plies, the 0° plies aligned with the loading direction.

2.2. Design of experiments: UQ&M input matrix

The uncertainty of the input parameters (the material and geometric variability and the presence of defects such as ply misalignment) is propagated to the notched strength to quantify their effect using the analysis models. To that end, a Monte-Carlo simulation (MCS) is carried out. The MCS relies on the repetition of random samples to obtain statistically representative numerical results. In other words, a sample is generated, where each specimen has different material properties, dimensions and ply misalignments.

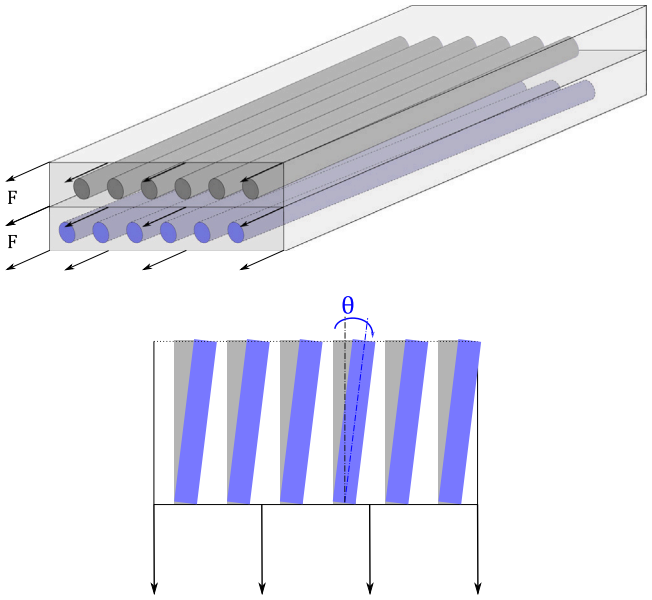

Fig. 2. Representation of the ply deviation. In gray the nominal ply with the fibers correctly aligned with the loading direction, whereas in blue is the deviated ply to account for ply misalignment. (For interpretation of the references to color in this figure legend, the reader is referred to the web version of this article.).

2.3. Uncertainty propagation

In this study, an analytical model based on FFM will be used to obtain fast predictions of the notched strength and to propagate the uncertainties. However, it is worth mentioning that, due to the simplifying assumptions that enable an analytical or semi-analytical treatment of the equilibrium equations, this model possesses some limitations, e.g., in the representation of stacking sequence effects and in the representation of ply misalignments (low fidelity model). Therefore, a FEM model will be also developed to capture the onset and propagation of the different damage mechanisms and to obtain more accurate results, but also computationally more expensive (high fidelity model).

2.3.1. Finite fracture mechanics model (low fidelity)

Low fidelity models are efficient tools that offer reasonably good predictions, subjected to particular limitations and constraints. The analytical model employed in this study is founded on the principles of finite fracture mechanics. Hence, it assumes that the propagation of a finite crack results from the simultaneous fulfillment of a stress-based and an energy-based criterion during crack propagation [17]:

$$\begin{cases} \frac{1}{l}\int_R^{R+l} \sigma_{xx}(0,y)dy = X^L \\ \int_R^{R+l} \mathcal{G}_I(a)da = \int_0^l \mathcal{R}(\Delta a)d\Delta a \end{cases} \tag{1}$$

where R is the hole radius, $\sigma_{xx}(0,y)$ is the stress distribution along the ligament section perpendicular to the loading direction, X^L is the laminate unnotched strength, $\mathcal{G}_I(a)$ is the mode I energy release rate (ERR) of a laminated plate with a central circular hole of radius R and two symmetric cracks propagating from the hole edge, $\mathcal{R}(\Delta a)$ is the $\mathcal{R}$-curve of the laminate and l is the crack extension at failure.

Furtado et al. [18] described a FFM model to calculate the notched strength of a CFRP laminate with only three material properties (the longitudinal Young's modulus (E_1), the fracture toughness ($\mathcal{G}_{IC}$) and the tensile strength (X_T)) based on the Trace theory and Master Ply concept [19] and on Omni Strain Last-Ply Failure envelopes [20]. Vallmajó et al. [2] utilized this analytical model with only three input material properties to evaluate the derivation of design allowables. Furthermore, it demonstrated the suitability of the model for accommodating different loading directions. Therefore, in this study, it will be employed to account for ply misalignment.

The analytical model was thoroughly validated for quasi-isotropic laminates [18]. More recently, Catalanotti et al. [21] developed a semi-analytical expression for the correction of the stress intensity factor for cracks emanating from circular holes taking into account the effect of geometry and orthotropy. Moreover, the orthotropy correction factor χ_i of each sub-laminate used in [18] was corrected [22,23]. This revisited FFM model was previously employed by Furtado et al. [24].

Nevertheless, this tool possesses some limitations that should be considered throughout the design process. First of all, the equations employed are only applicable to balanced laminates. Secondly, it does not account for delamination, i.e., it cannot predict the matrix failure between layers. Lastly, failure must be concentrated on a unique plane. In other words, it is assumed that damage initiates and propagates within the same plane.

The low fidelity model is implemented in a Python script which can be executed with minimal computational resources, enabling the rapid generation of a large amount of data within a short period of time.

2.3.2. Finite element model (high fidelity)

To overcome the constraints of the low fidelity model, a numerical model has been developed to determine the notched strength and investigate the failure mechanisms that lead to laminate failure. These FEM models rely on constitutive models developed through the principles of continuum damage mechanics. These models aid in characterizing the behavior of CFRP under different loading conditions and are capable of predicting damage initiation and evolution. Therefore, they enable the prediction not only of notched strength but also the understanding of the failure mechanisms that lead to the specimen failure.

The high fidelity model is developed in the finite element software ABAQUS/Explicit 6.14-2 [25]. The modeling strategy used to model the OH tensile specimen follows Furtado et al. [26] in which a convergence analysis was performed to validate the mesh discretization and modeling strategy. Thus, the same simulation approach is applied in this work. Each ply is simulated using one 8-node linear brick reduced integration element (C3D8R) along the ply thickness and the plies are connected by 0.01 mm thick COH3D8 Abaqus cohesive elements. The laminate is clamped on one end while on the other a smooth displacement is applied to all nodes at the boundary (see Fig. 3). The mechanical behavior of the material is defined using a VUMAT subroutine which integrates an extension of the continuum damage mechanics model proposed by Maimíet al. [27]. In addition, a cohesive zone model is incorporated to predict delamination onset and propagation, following Turon et al. [28]. The integration of these models follows the work of Furtado et al. [26] for a comprehensive approach for the analysis of the OH strength of composite laminates.

2.4. Virtual calculation of notched strength uncertainties

To address the influence of uncertainties and defects, a single, deterministic calculation is not enough. Consequently, statistically-based material parameters, known as design allowables, are used in the industry. The most commonly employed in the aeronautical industry is the B-basis value as proposed in the CMH-17 [1], which corresponds to the 95% lower confidence bound on the 10th percentile. The following procedure outlines the determination of the B-value implemented in this work:

1. Calculate notched strength values from multiple specimens, accounting for material and geometric uncertainties, as well as ply misalignment defects.

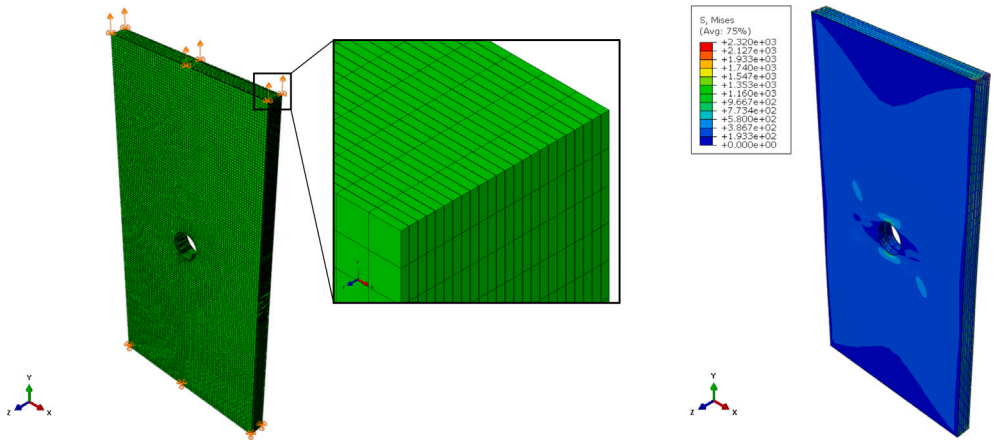

Fig. 3. Modeling strategy of the OH specimen pointing out the mesh and boundary conditions and the results obtained in a representative simulation.

Table 1
Material properties for the low fidelity model [2].

Input parameter for FEM analysis	Unit	Mean	CoV (%)
Ply longitudinal Young's modulus, E_1	GPa	171.42	1.39
Ply longitudinal tensile strength, X_T	GPa	2323.47	5.48
Ply longitudinal steady state fracture toughness, $\mathcal{R}_{ssT}$	N/mm	206.75	11.43

Table 2
Material properties for the high fidelity model [29].

Input parameter for FEM analysis	Unit	Mean	CoV (%)
Young's modulus in fiber direction, E_1	GPa	171.42	1.39
Young's modulus in matrix direction, E_2	GPa	9.08	1.03
Poisson's ratio in 1–2 plane, ν_{12}	–	0.32	6.18
Poisson's ratio in 2–3 plane, ν_{23}	–	0.487	2.20
Shear modulus in the 1–2 plane, G_{12}	MPa	5290	2.53
Longitudinal tensile strength, X_T	MPa	2323.50	5.5
Ratio of the first branch of tensile cohesive law, f_{XT}	–	0.40	8
Longitudinal compressive strength, X_C	MPa	1200.10	12.1
Ratio of the first branch of compressive cohesive law, f_{XC}	–	0.20	8
Transverse tensile strength, Y_T	MPa	62.30	8.5
Transverse compressive strength, Y_C	MPa	253.70	10.2
Longitudinal shear strength, S_L	MPa	92.30	3.1
Longitudinal tensile fracture toughness, $\mathcal{G}_{XT}$	kJ/m^2	133.30	5
Ratio of $\mathcal{G}_{XT}$ dissipated in the first branch, $f_{\mathcal{G}_{XT}}$	–	0.30	8
Longitudinal comprehensive fracture toughness, $\mathcal{G}_{XC}$	kJ/m^2	61	2
Mode I interlaminar fracture toughness, $\mathcal{G}_{Ic}$	kJ/m^2	0.28	5
Transverse tensile fracture toughness, $\mathcal{G}_{YT}$	kJ/m^2	0.28	5
Transverse compressive fracture toughness, $\mathcal{G}_{YC}$	kJ/m^2	1.31	2
Mode II interlaminar fracture toughness, $\mathcal{G}_{IIc}$	kJ/m^2	0.79	18
Transverse shear fracture toughness, $\mathcal{G}_{SL}$	kJ/m^2	0.79	18
Strength in pure mode I, $Coh-t3$	MPa	62.30	5
Strength in pure mode II, $Coh-t1$	MPa	92.30	5
B-K exponent parameter for mixed mode propagation, BK_η	–	1.45	10

2. Identify and delete any potential outliers within the sample following the CMH-17 approach. An outlier is a result that exhibits a quantity of interest that is much lower or much higher than most other observations. Therefore, they are assumed to be erroneous values. In that case, the maximum normed residual method is used to screen and identify these extreme values. This method consists in comparing the deviation between each value and the sample mean considering the sample standard deviation.
3. Compute the 10th percentile with 95% confidence. This value is derived from the empirical cumulative density function (ECDF). However, it is important to note that obtaining an ECDF typically requires large sample sizes [2]. This may not be practical for FEM analysis due to the associated computational costs [3]. Therefore, for high fidelity analysis, the B-value is determined following the CMH-17 specifically and also compared with the 10th percentile obtained from the ECDF of the data generated.

3. Case study

This section describes the ply properties used in the low and high fidelity uncertainty propagation analyses and the uncertainties in the material properties, in the geometry and in the ply deviations (or misalignments).

3.1. Material selection and material properties

The proposed methodology can be applied to any CFRP. In this study, the IM7/8552 carbon/epoxy system is considered due to the availability of material properties and due to the fact that the models considered in the OH strength calculations had been previously validated with this material system. As mentioned in Section 2.3.1, the analytical model only requires three material properties which are summarized in Table 1. However, for the FEM analysis, more parameters are needed to account for the elastic, strength and fracture

properties related to the main orthotropy axes of the material system (see Table 2). In both cases, it is assumed that the material properties follow a normal distribution.

Concerning the geometry, a rectangular specimen with a central circular hole, subjected to tensile loading, is considered. The hole diameter-to-width ratio ($2R/W$) is 1/6 and the hole diameter is 6 mm [30]; however, any alternative geometry could be considered. Furthermore, for a better understanding of the impact of ply misalignment, different configurations of balanced laminates, each consisting of 24 plies, were studied:

- Quasi-isotropic (QI) laminate: $[90, 0, -45, 45]_{3s}$
- Soft laminate: $[45, 90, -45, 90, 45, 90, -45, 0, 45, 90, -45, 90]_s$
- Hard laminate: $[45, 0, -45, 0, 45, 90, -45, 0, 45, 0, -45, 0]_s$

3.2. Discretization of defects

Ply misalignment refers to a deviation in the orientation of each individual ply within a composite structure. Instead of assuming a deterministic layup, variability in each ply orientation was introduced. While many companies agree that ply misalignment should be kept between 2° and 3° [8,10,31], it is noteworthy that deviations of up to 7° have been identified by the industry. To provide a comprehensive assessment of the effect of ply misalignment, this study considers deviations around 7°, although it is acknowledged as an extreme value. Ply misalignment is commonly assumed to follow a normal distribution. However, it can also be conceptualized as a tolerance which is randomly, uniformly distributed. Moreover, in cases where errors occur in the template alignment during the ply cutting or in the placement of each ply to build the laminate, this can introduce a bias deviation, leading to a specific ply deviation in all plies or just those using the incorrect template. Therefore, in this study, three different scenarios of misalignment are considered:

- Normal distributed ply misalignment with a STDV of 7° and a mean value of 0°: $\theta_i = N(0°, 7°)$.
- Uniformly distributed ply misalignment in the range $\theta_i = [-2 \times 7°, +2 \times 7°]$.
- A bias ply deviation of 7° for the 0° plies, in addition to a normal distributed ply misalignment with a STDV of 7°: $\theta_i = N(7°, 7°)$ for the 0° plies and $\theta_i = N(0°, 7°)$ for all the other plies.

Moreover it is worth mentioning that different considerations were applied for each modeling approach, linked to the constraints of the low fidelity model:

- The FFM model is valid for balanced laminates. Therefore, the ply deviations (θ_i) cannot be completely random for all plies in the laminate. Instead, only some ply misalignments are randomly generated, while some need to be adjusted accordingly to maintain the laminate balanced. For instance, for the QI laminate, only 5 different misalignment angles (θ_i) were introduced to ensure that the laminate remains balanced: $[90+\theta_1, 0+\theta_2, -45+\theta_3, 45-\theta_3, 90-\theta_1, 0-\theta_2, -45+\theta_4, 45-\theta_4, 90, 0, -45+\theta_5, 45-\theta_5]_s$.
- The FEM model does not have those constraints. Therefore, a random deviation has been considered for each ply in this case using either the normal distribution, the uniform distribution or the bias ply deviation.

4. Results and discussion

4.1. Results comparison: FFM vs. FEM

Before accounting for the effect of ply misalignment, the results obtained from the low and high fidelity models are compared with experimental results available for the QI laminate. The comparison between the analytical predictions, accounting for both material and geometric variability, and the experimental results was reported in [2]. Nevertheless, as mentioned in Section 2.3.1, the analytical model has been revisited to consider the orthotropy of the laminate and it incorporates a corrected χ_i definition [24]. The implementation is used to calculate 10 000 predictions (following the same strategy presented in [2]) to predict the mean and STDV results. The FFM model is still subjected to certain constraints. Hence, in this study, FEM analysis is also conducted to provide more accurate predictions of damage onset and propagation. The modeling strategy based on FEM is used to generate 200 simulations to predict the mean value and STDV. The comparison of both results with experiments is presented in Fig. 4.

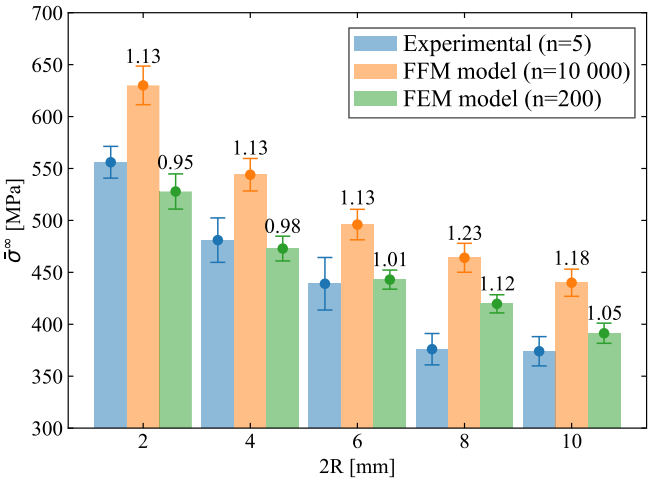

Fig. 4. Comparison of the experimental results [32] with the analytical and FEM results. The values presented correspond to the ratio between the predicted mean value and the mean experimental value. (For interpretation of the references to color in this figure legend, the reader is referred to the web version of this article.).

The results show that the analytical model predicts higher notched strength compared with the experimental results, with errors ranging between 13% and 23% according to the studied diameter. Yet, it is important to highlight that these analytical models are fast tools that aid in understanding the behavior of the composite structure and provide a first approximation of the notched strength, which can be valuable for preliminary assessments. The results obtained using the high fidelity model exhibit a closer agreement with experimental data. As mentioned earlier, the low fidelity model has certain limitations and constraints. Notably, it does not account for delamination, leading to significantly higher values in the analytical model results. However, it is evident that delamination plays a significant role, as illustrated in Fig. 5.

Although the analytical model provides higher over-predictions, both methods predict the notched strength of CFRP with reasonable accuracy, validating both approaches. In a detailed design stage, if more precision is required, the high-fidelity model is recommended. However, for preliminary design, when fast predictions are necessary, the low-fidelity model emerges as a powerful tool.

4.2. Determination of the sample size to account for ply misalignment

Following Vallmajó et al. [2], it has been demonstrated that, for large samples, the B-basis value can be directly predicted as the 10th percentile. This is due to the minimal deviation in such cases, so the 95% lower confidence bound tends to the mean value. Considering this insight, this section incorporates a comprehensive analysis to determine the minimum number of samples for which the B-value can be approximated as the 10th percentile when also considering ply misalignment. Fig. 6 shows the error bars corresponding to one STDV of the mean values and of the B-values of the notched strength calculated from 10 groups of samples of n predictions.

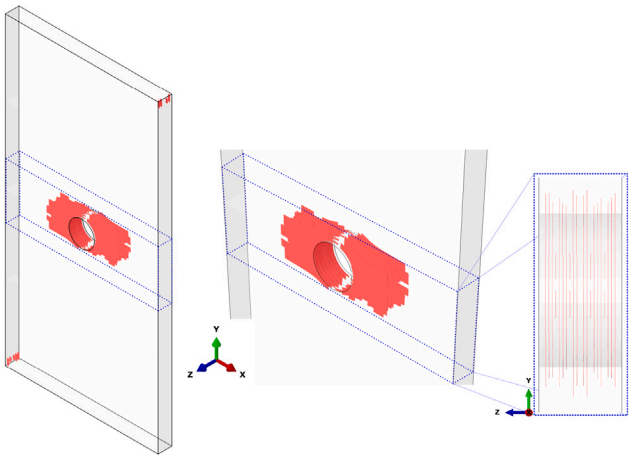

Fig. 5. Delamination (in red), i.e., inter-ply damage, at the peak load predicted by FEM analysis for the QI laminate. Delamination (in red) corresponds to the elements with a cohesive damage variable (SDEG) equal to 1. (For interpretation of the references to color in this figure legend, the reader is referred to the web version of this article.).

The results demonstrate that when accounting for fiber misalignment, a sample size of 10 000 predictions is high enough for uncertainty propagation considering a normal distribution or a uniform distribution.

Regarding the FEM analysis, the sample size (n) was reduced due to the significantly higher computational costs. This reduction was determined following a balance between the accuracy of the results and the computational cost. Fig. 7 illustrates the predictions using different sample sizes, up to a maximum of 300 virtual specimens.

Consequently, a sample size of 200 values was considered suitable for the FEM analysis, since the mean value is close to the one obtained with 300 samples. Moreover, the low STDV suggests that a plateau has likely been reached.

4.3. Effect of random ply misalignment

Both methods are now used to determine the effect of ply misalignment in all the scenarios considered in this study. The ECDF of the results, the histogram, and the B-value prediction obtained from the FEM model and the analytical model are presented in Fig. 8 for the QI laminate and Fig. 9 for the hard and soft laminates.

As expected, when comparing the different laminates, the QI results fall between the hard laminate, which achieved the highest notched strength, and the soft laminate, with the lowest values. Fig. 10 presents the stress–displacement curves for the three studied laminates and the main failure mechanisms. As discussed in Section 4.1, the analytical predictions are higher than the numerical results because they solely consider fracture within the same plane, without accounting for delamination or other subcritical damage mechanisms. However, for the soft laminate, the prediction from the low fidelity model is lower than the value predicted by the high fidelity analysis. This can be explained by the presence of very few 0° plies, which are the main responsible for bearing the applied load, and a significant role of delamination and other subcritical damage mechanisms. In fact, the delaminated area of the soft laminate is 50% larger than that of the hard laminate, and 35% larger than that of the QI laminate. Consequently, the distribution of the notched strength of the soft laminate obtained using the analytical model is not correct as can be identified in Figs. 8 and 9 where the ECDF when employing the analytical models exhibits a bimodal shape.

It can be concluded that, beyond the application domain, there are large differences between the analytical and the FEM results, whether in the nominal case or the stochastic analysis. This underscores the importance of recognizing the limitations of analytical models, even though they are valuable tools.

With both approaches, analytically and numerically, the B-value when incorporating ply misalignment is lower than when only considering material and geometric variability. That can be attributed to the increase in the STDV, i.e., the ECDF is wider. Moreover, in the analytical analysis, the distribution shifts to the left side when accounting for ply deviation, resulting in a lower mean value. Interestingly, despite the analytical nominal values being higher than those obtained by FEM, the B-values for the QI and hard laminates are more conservative. In contrast, in the FEM analysis, the mean values remain almost constant for all scenarios, except when introducing a bias factor. In that last scenario, the mean value is lower when accounting for ply misalignment than when only considering material and geometric variability. The lowest B-value is always obtained when considering all the uncertainties simultaneously. This implies that each uncertainty contributes to the overall variability. However, the relationship of the density function when considering only one uncertainty versus the density function when considering that uncertainty along with another one does not follow a straightforward pattern.

a) Normal distribution

b) Uniform distribution

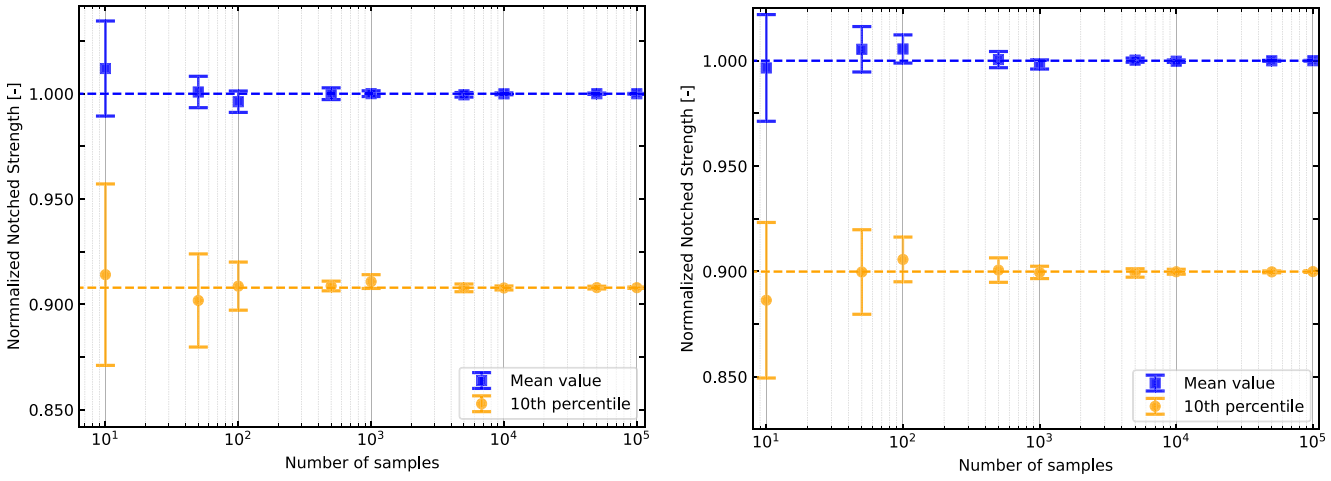

Fig. 6. Average OH strength and 10th percentile from $N = 10$ samples of different size n using the analytical approach. Each sample considers material variability, geometric tolerances and random ply misalignments following a normal and uniform distribution, respectively. (For interpretation of the references to color in this figure legend, the reader is referred to the web version of this article.).

Table 3
Comparison of the analytical and FEM results considering material and geometric variability only.

Case study	Analysis	Nominal value [MPa]	Mean value [MPa]	CoV [%]	10th percentile ECDF [MPa]	B-value CMH-17 [MPa]	B-value calc. difference [%]	B-value-to-mean ratio [%]	Ratio calc. difference [%]
QI laminate	FEM	442	443	2.1	431	427	−11.5	97	0.9
	Anal	497	496	2.9	477	476		96	
Hard laminate	FEM	569	564	2.6	547	543	−19.0	95	−0.4
	Anal	674	673	3.0	646	646		96	
Soft laminate	FEM	296	295	1.7	288	287	26.5	97	23.6
	Anal	285	266	11.3	211	211		74	

Table 4
Comparison of the analytical and FEM results considering the effect of ply misalignment only.

Case study	Analysis	Nominal value [MPa]	Mean value [MPa]	CoV [%]	10th percentile ECDF [MPa]	B-value CMH-17 [MPa]	B-value calc. difference [%]	B-value-to-mean ratio [%]	Ratio calc. difference [%]
QI laminate Normal, 7°	FEM	442	441	3.9	419	418	−4.5	97	7.0
	Anal	497	483	7.2	438	437		88	
QI laminate Uniform, 7°	FEM	442	445	5.1	415	412	−3.9	93	7.6
	Anal	497	477	7.7	429	428		86	
QI laminate Bias 7° + Normal, 7°	FEM	442	437	5.0	408	405	−2.5	92	8.9
	Anal	497	452	6.4	416	415		84	
Hard laminate, Normal, 7°	FEM	569	566	2.9	544	542	−9.6	95	7.5
	Anal	674	643	5.6	595	594		88	
Soft laminate Normal, 7°	FEM	296	301	7.8	271	268	3.0	91	−0.8
	Anal	285	265	13.9	261	260		91	

Table 5
Comparison of the analytical and FEM results when considering material and geometric variability and ply misalignments.

Case study	Analysis	Nominal value [MPa]	Mean value [MPa]	CoV [%]	10th percentile ECDF [MPa]	B-value CMH-17 [MPa]	B-value calc. difference [%]	B-value-to-mean ratio [%]	Ratio calc. difference [%]
QI laminate Normal, 7°	FEM	442	441	5.1	413	408	−6.1	92	5.6
	Anal	497	481	7.9	434	433		87	
QI laminate Uniform, 7°	FEM	442	440	6.3	406	400	−5.3	90	6.4
	Anal	497	474	8.9	422	421		85	
QI laminate Bias 7° + Normal, 7°	FEM	442	436	5.5	407	401	−1.7	91	9.5
	Anal	497	447	7.9	409	408		82	
Hard laminate, Normal, 7°	FEM	569	561	3.9	530	529	−11.5	93	5.8
	Anal	674	643	6.2	591	590		88	
Soft laminate Normal, 7°	FEM	296	300	7.5	269	267	15.4	90	12.1
	Anal	285	279	13.0	228	226		79	

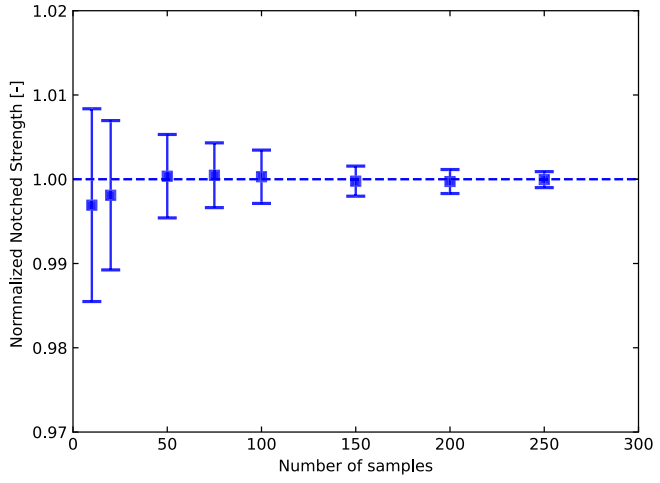

Fig. 7. Average OH strength from $N = 10$ samples of different size n using the FEM approach. Each sample considers material variability, geometric tolerances and random ply misalignments following a normal and uniform distribution, respectively.

To better discuss the results obtained numerically and analytically, Tables 3–5 summarize the different deterministic and statistical measures of the predicted notched strength.

As introduced by Cózar et al. [3], the B-value calculated following the CMH-17 approach tends to be more conservative, especially with small sample sizes. Consequently, in the FEM analysis, where 200 simulations are considered, the B-value computed using the CMH-17 approach is lower than the one obtained from the ECDF. Conversely, for the low fidelity model, with 10 000 simulations being used, the predicted B-values using both approaches are very close.

When only accounting for material and geometric variability, the difference between the B-values computed using the CMH-17 approach from both solutions exhibits a large discrepancy, with differences above 10%. This difference is even more pronounced for the soft laminate, because the analytical model does not provide good predictions. Nevertheless, when evaluating the ratio between the B-value and the mean value, the difference between the two cases is lower than 1%. Therefore, a valuable approach would be to predict the nominal value through the high fidelity analyses while determining the B-value by calculating the B-value-to-mean ratio with the analytical model.

When only addressing ply misalignment, the error in the predicted B-value decreases. However, the analytical model predicts a notable

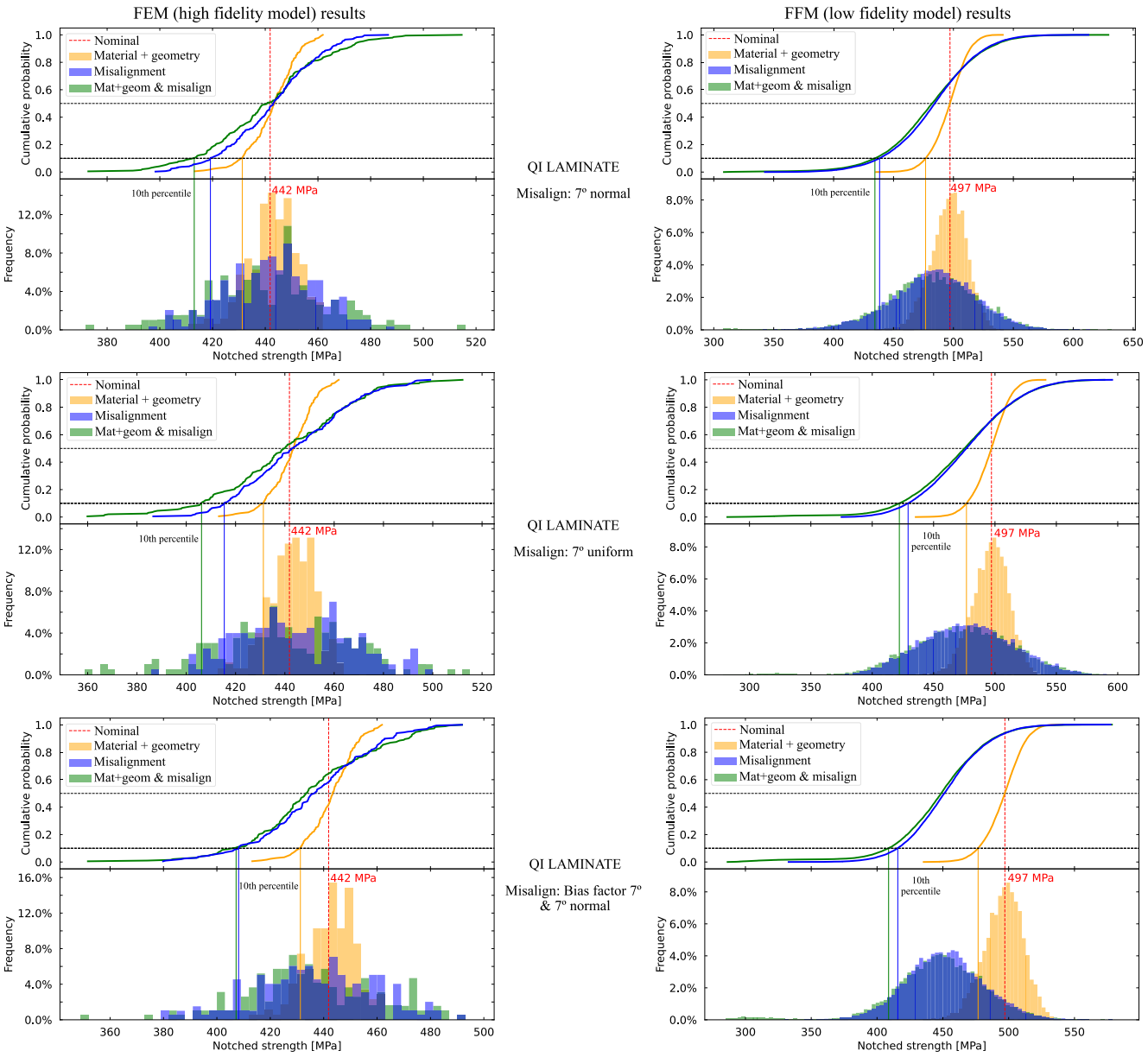

Fig. 8. Distributions of the notched strengths and B-value for the quasi-isotropic (QI) laminate obtained by the FEM (left) and analytical models (right). (For interpretation of the references to color in this figure legend, the reader is referred to the web version of this article.).

decrease in the mean values, while the FEM outcomes exhibit similar mean values, except when introducing ply misalignment and a bias factor in the 0° plies. Furthermore, the STDV due to ply misalignments obtained from high fidelity analysis is higher than the STDV when considering material and geometric variability only. Consequently, the difference between the B-value-to-mean ratios obtained from the analytical or FEM models increases when considering ply misalignments.

Comparing the results when the misalignment is modeled with a normal or a uniform distribution, the latter exhibits larger variability due to the wider range of variance, resulting in a lower B-value. Moreover, when introducing a bias misalignment in all 0° plies, the mean value decreases leading to the lowest predictions.

Finally, when considering all differences, the distinctions between both analyses remain equivalent to considering ply misalignment only. In other words, the difference between the B-value-to-mean ratios obtained from the low and high fidelity models increases when considering ply deviation. This can be attributed to the impact of the fiber deviation on the damage mechanisms that trigger specimen failure. To further investigate this, a comparison between the stress–displacement curves and the main failure mechanisms for the QI laminate is presented in Fig. 11, considering material and geometry variability alone and also accounting for ply misalignment following a normal distribution.

For a more accurate analysis, the case with the highest strength (obtained when only considering material and geometry variability) is compared against the lowest one (when ply deviation is also taken into account). The results demonstrate a reduction in strength around 25% due to the absence of 0° plies that can carry the applied load. Moreover, the comparison between fiber, matrix and inter-ply damage clearly shows that the specimen failure is more catastrophic when introducing ply misalignment, but without following a clear pattern. However, when assuming the nominal laminate, there is fiber damage around the hole in the 0° plies, as expected [32]. Furthermore, this damage triggers delamination on the adjacent plies, leading to final failure of the specimen.

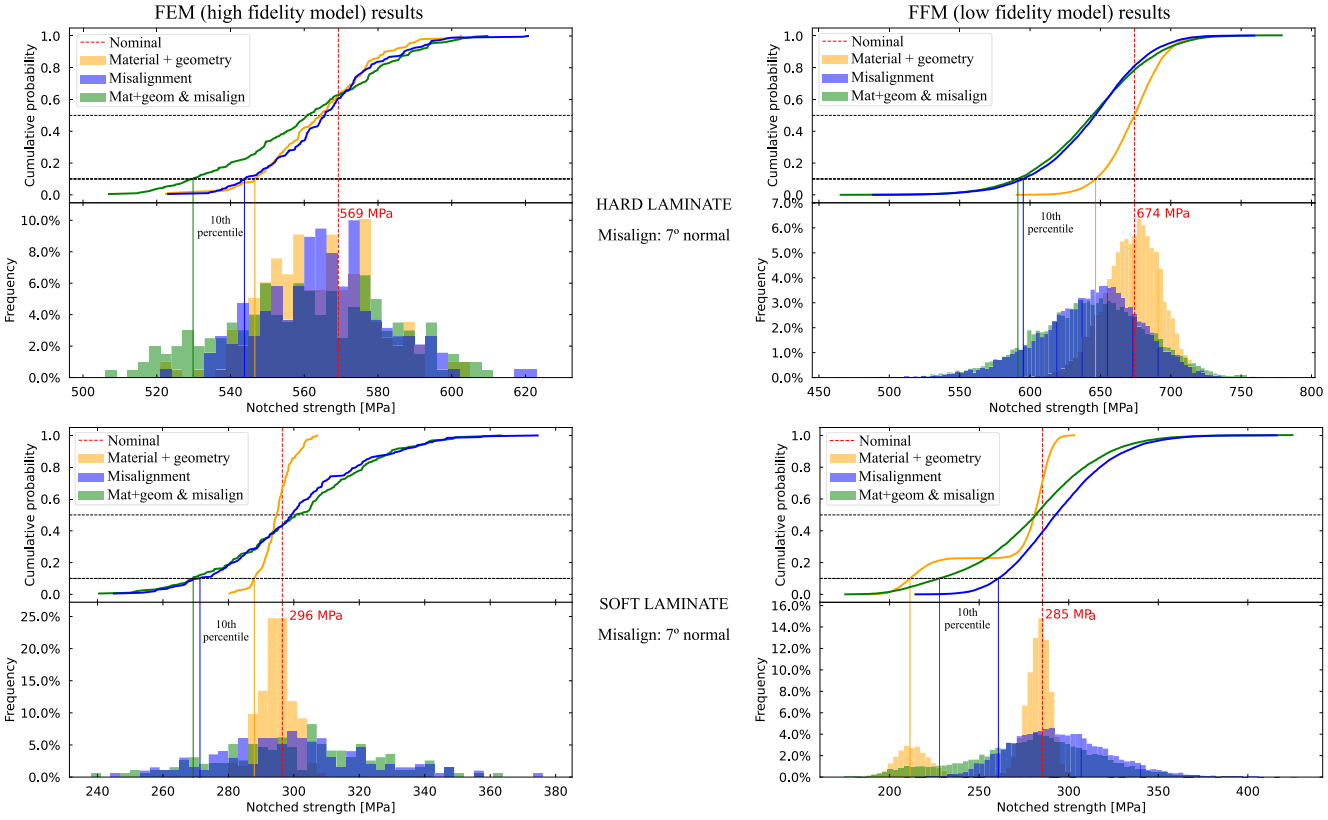

Fig. 9. Distributions of the notched strengths and B-value for the hard and soft laminate obtained by the FEM (left) and analytical models (right). (For interpretation of the references to color in this figure legend, the reader is referred to the web version of this article.).

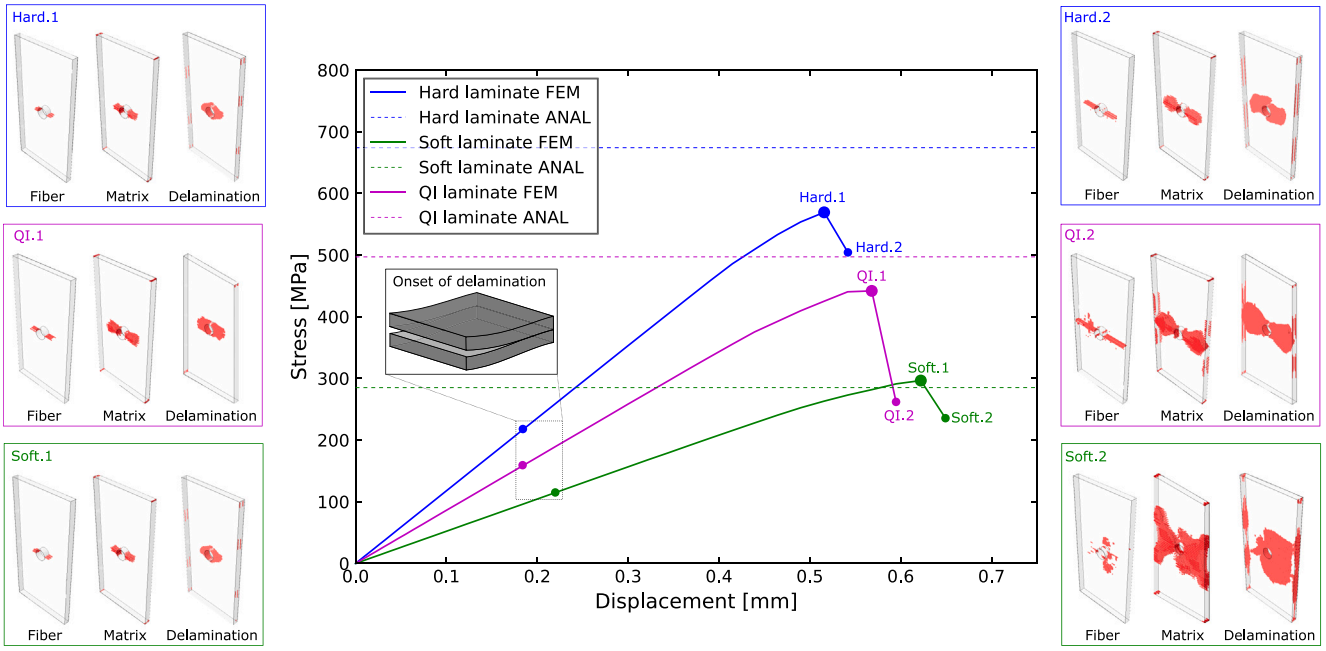

Fig. 10. Stress–displacement curve and failure mechanisms (fiber and matrix intra-ply damage and delamination, shown in red) predicted for the QI, soft and hard laminates. Fiber damage corresponds the elements with a fiber damage variable (d_1) equal to 1; matrix damage corresponds to the elements with a matrix (d_2) and shear (d_6) damage variable equal to 1; delamination corresponds to the elements with a cohesive damage variable (SDEG) equal to 1. (For interpretation of the references to color in this figure legend, the reader is referred to the web version of this article.).

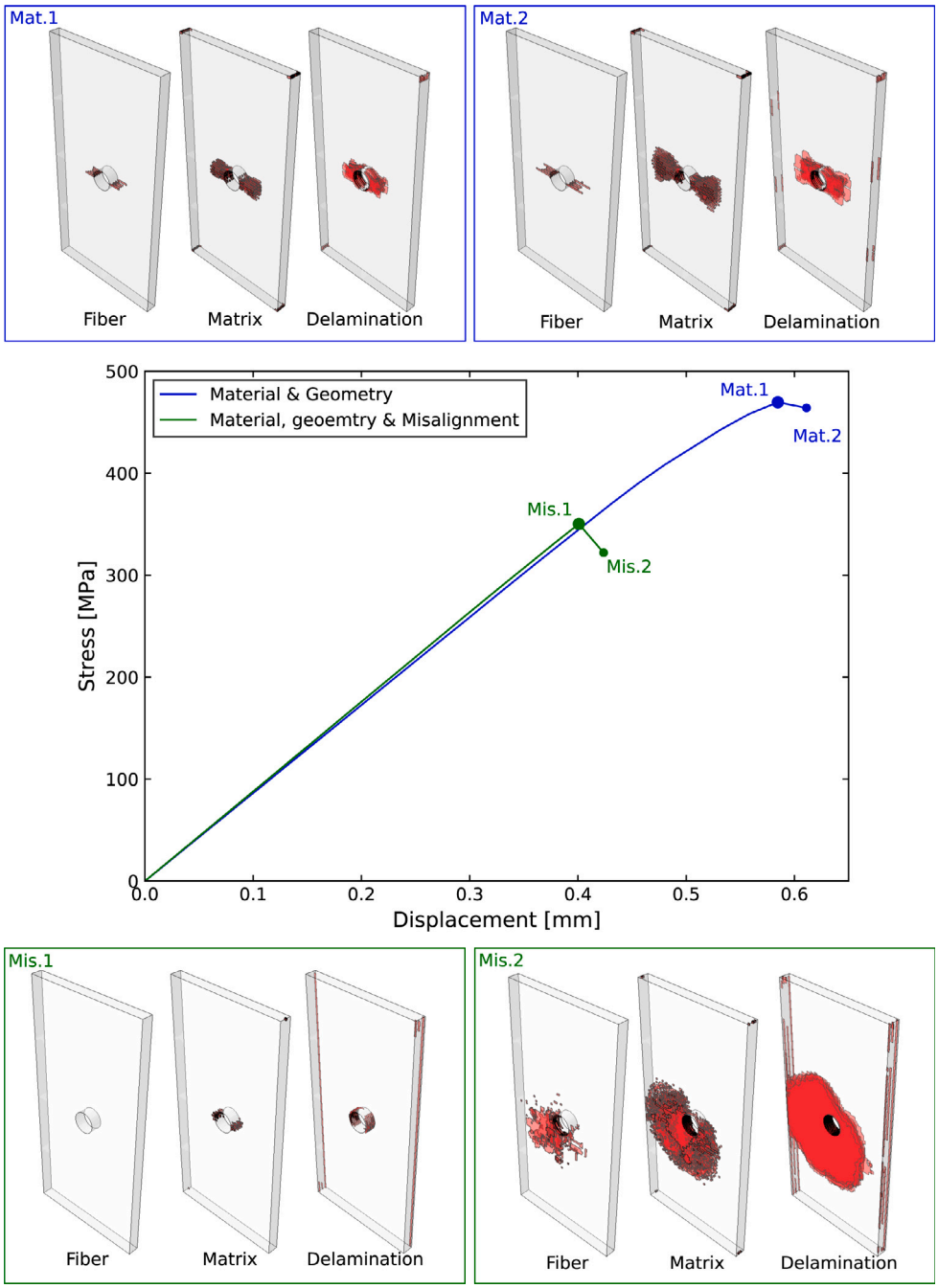

Fig. 11. Stress–displacement curve and failure mechanisms (fiber and matrix intra-ply damage and delamination shown in red) predicted for the QI laminate when considering material and geometry variability (highest value in blue) and when also accounting for ply misalignment following a normal distribution (lowest value in green). Fiber damage corresponds the elements with a fiber damage variable (d_1) equal to 1; matrix damage corresponds to the elements with a matrix (d_2) and shear (d_6) damage variable equal to 1; delamination corresponds to the elements with a cohesive damage variable (SDEG) equal to 1. (For interpretation of the references to color in this figure legend, the reader is referred to the web version of this article.).

5. Conclusions

In this study, the use of analytical and numerical modeling and simulation approaches was exploited to assess the effect of meso-scale defects, specifically, ply misalignments in the calculation of design allowables of notched specimens. Different virtual specimens, considering both material and geometric variability as well as ply deviations were studied. This analysis involved the application of an analytical model and a FE numerical simulation employing the appropriate mechanical constitutive model. Therefore, a precise methodology has been described for the propagation of the aforementioned uncertainties to determine the notched strength of different laminates: quasi-isotropic, hard and soft.

Based on the nominal OH strength, the hard laminate, which is mainly composed of 0° plies, exhibits the highest resistance compared with the QI and soft laminates, which, in contrast, exhibit the lowest strengths. The analytical predictions for the hard and quasi-isotropic laminates are in good agreement with the numerical values, aligning well with the experimental data available for the QI laminate. In contrast, the soft laminate predictions with the analytical model are

less accurate, due to the omission of delamination and other subcritical damage mechanisms, which, as revealed in the FEM analysis, play a major role on the failure development process. When introducing geometric and material variability, the uncertainty increases while the mean value remains constant. Moreover, when accounting for ply deviation, the uncertainties further increase. When comparing the predictions of the analytical and FEM models, the B-value-to-mean ratio are in good agreement, although the differences increase when introducing ply deviation due to changes in the damage mechanisms triggered by the absence of 0° plies.

To sum up, this study underscores the ability of analytical models, which are fast tools, to predict the notched strength while accounting for material and geometric variability, as well as ply misalignment. These analytical tools can be valuable as a guideline in the preliminary design of composite structures. On the other hand, FEM simulations provide more accurate results and offer insights into the failure mechanisms responsible for laminate failure. Therefore, it is crucial to establish the necessary level of accuracy required during the design stage. Additionally, considering a hybrid approach may be useful, given that FEM predictions offer more accuracy in determining the mean values, while fast analytical models can be used to propagate uncertainties and to determine the allowables thanks to good predictions of the allowable-to-mean ratios.

CRediT authorship contribution statement

O. Vallmajó: Writing – review & editing, Writing – original draft, Visualization, Validation, Supervision, Software, Resources, Methodology, Investigation, Formal analysis, Data curation, Conceptualization. **M. Descamps:** Writing – review & editing, Visualization, Software, Methodology. **A. Arteiro:** Writing – review & editing, Validation, Supervision, Methodology, Investigation, Formal analysis, Conceptualization. **A. Turon:** Writing – review & editing, Supervision, Project administration, Methodology, Funding acquisition, Formal analysis, Conceptualization.

Declaration of competing interest

The authors declare that they have no known competing financial interests or personal relationships that could have appeared to influence the work reported in this paper.

Data availability

The data that has been used is confidential.

Acknowledgments

OV acknowledges the support of the Catalan Government, under the Grant 2020FI B2 00110. AT and OV gratefully acknowledge the funding of the Project RTI 2018-099373-B-100, co-financed by the Spanish Government (Ministerio de Economia *y* Competitividad) and the European Social Fund. AT acknowledges the Generalitat de Catalunya for the ICREA Academia prize 2022. This work has been conducted within the framework of the CAELESTIS project, funded by the European Climate, Infrastructure and Environment Executive Agency (CINEA) under grant agreement No. 101056886. Views and opinions expressed are however those of the author(s) only and do not necessarily reflect those of CINEA. Neither the European Union nor the granting authority can be held responsible for them. Open Access funding provided thanks to the CRUE-CSIC agreement with Elsevier.

References

[1] Handbook M. MIL-HDBK-17-1F: Composite materials handbook. In: Volume 1-polymer matrix composites guidelines for characterization of structural materials.
[2] Vallmajó O, Cózar I, Furtado C, Tavares R, Arteiro A, Turon A, Camanho P. Virtual calculation of the B-value allowables of notched composite laminates. Compos Struct 2019;212:11–21.
[3] Cózar I, Turon A, González E, Vallmajó O, Sasikumar A. A methodology to obtain material design allowables from high-fidelity compression after impact simulations on composite laminates. Composites A 2020;139:106069.
[4] Catalanotti G. Navigating the unknown: Tackling high-dimensional challenges in composite damage modeling with bootstrapping and Bayesian uncertainty quantification. Compos Sci Technol 2024;248:110462.
[5] Sebaey T, Catalanotti G, Lopes C, O'Dowd N. Computational micromechanics of the effect of fibre misalignment on the longitudinal compression and shear properties of UD fibre-reinforced plastics. Compos Struct 2020;248:112487.
[6] Potter K, Langer C, Hodgkiss B, Lamb S. Sources of variability in uncured aerospace grade unidirectional carbon fibre epoxy preimpregnate. Composites A 2007;38(3):905–16.
[7] Sebaey T, Catalanotti G, O'Dowd N. A microscale integrated approach to measure and model fibre misalignment in fibre-reinforced composites. Compos Sci Technol 2019;183:107793.
[8] Hinckley M. Statistical evaluation of the variation in laminated composite properties resulting from ply misalignment. In: Advances in optical structure systems. vol. 1303, International Society for Optics and Photonics; 1990, p. 497–511.
[9] Arao Y, Koyanagi J, Utsunomiya S, Kawada H. Effect of ply angle misalignment on out-of-plane deformation of symmetrical cross-ply CFRP laminates: Accuracy of the ply angle alignment. Compos Struct 2011;93(4):1225–30.
[10] Steeves J, Pellegrino S. Post-cure shape errors of ultra-thin symmetric CFRP laminates: Effect of ply-level imperfections. Compos Struct 2017;164:237–47.
[11] Liu Q, Cai Y, Liu X, Yang Z, Jiang S, Leng S. Influence of the ply angle deviation on the out-of-plane deformation of the composite space mirror. Appl Compos Mater 2019;26:897–911.
[12] Thompson SJ, Bichon S, Grant RJ. Influence of ply misalignment on form error in the manufacturing of CFRP mirrors. Opt Mater Express 2014;4(1):79–91.
[13] Cheng L, Gong P, Wang Q, Zou M, Zhang Y, Liu Z. Effects of ply thickness deviation and ply angle misalignment on the surface accuracy of CFRP laminates. Compos Struct 2021;270:114073.
[14] Tanaka S, Ikeda T, Senba A. Sensitivity analysis of thermal deformation of CFRP laminate reflector due to fiber orientation error. J Mech Sci Technol 2016;30:4423–6.
[15] Vallmajó O, Arteiro A, Guerrero J, Melro A, Pupurs A, Turon A. Micromechanical analysis of composite materials considering material variability and microvoids. Int J Mech Sci 2023;108781.
[16] Nguyen MH, Vijayachandran AA, Davidson P, Call D, Lee D, Waas AM. Effect of automated fiber placement (AFP) manufacturing signature on mechanical performance of composite structures. Compos Struct 2019;228:111335.
[17] Camanho P, Erçin G, Catalanotti G, Mahdi S, Linde P. A finite fracture mechanics model for the prediction of the open-hole strength of composite laminates. Composites A 2012;43(8):1219–25.
[18] Furtado C, Arteiro A, Bessa M, Wardle B, Camanho PP. Prediction of size effects in open-hole laminates using only the Young's modulus, the strength, and the R-curve of the 0° ply. Composites A 2017;101(AAA):306–17.
[19] Tsai SW, Melo JDD. An invariant-based theory of composites. Compos Sci Technol 2014;100:237–43.
[20] Tsai SW, Melo JDD. A unit circle failure criterion for carbon fiber reinforced polymer composites. Compos Sci Technol 2016;123:71–8.
[21] Catalanotti G, Salgado RM, Camanho PP. On the stress intensity factor of cracks emanating from circular and elliptical holes in orthotropic plates. Eng Fract Mech 2021;252:107805.
[22] Bao G, Ho S, Suo Z, Fan B. The role of material orthotropy in fracture specimens for composites. Int J Solids Struct 1992;29(9):1105–16.
[23] Corrigenda. Int J Solids Struct 1992;29(16):2115.
[24] Furtado C, Pereira L, Tavares RP, Salgado M, Otero F, Catalanotti G, Arteiro A, Bessa MA, Camanho PP. A methodology to generate design allowables of composite laminates using machine learning. Int J Solids Struct 2021;233:111095.
[25] User's manual, 6.14-2. Pawtucket, RI, USA: ABAQUS Inc.; 2014.
[26] Furtado C, Catalanotti G, Arteiro A, Gray P, Wardle B, Camanho P. Simulation of failure in laminated polymer composites: Building-block validation. Compos Struct 2019;226:111168.
[27] Maimí P, Camanho PP, Mayugo J, Dávila C. A continuum damage model for composite laminates: Part I constitutive model. Mech Mater 2007;39(10):897–908.
[28] Turon A, González E, Sarrado C, Guillamet G, Maimí P. Accurate simulation of delamination under mixed-mode loading using a cohesive model with a mode-dependent penalty stiffness. Compos Struct 2018;184:506–11.

[29] Sasikumar A, Turon A, Cózar IR, Vallmajó O, Casero JC, De Lozzo M, Abdel-Monsef S. Sensitivity analysis methodology to identify the critical material properties that affect the open hole strength of composites. J Compos Mater 2023;57(10):1791–805.
[30] American Society for Testing, Materials P. Filadelfia ASTM D5766-D5766M-11: standard test method for open-hole tensile strength of polymer matrix composite laminates. ASTM; 2011.
[31] Potter K, Khan B, Wisnom M, Bell T, Stevens J. Variability, fibre waviness and misalignment in the determination of the properties of composite materials and structures. Composites A 2008;39(9):1343–54.
[32] Camanho PP, Maimí P, Dávila C. Prediction of size effects in notched laminates using continuum damage mechanics. Compos Sci Technol 2007;67(13):2715–27.